KTH Electrical Engineering

Analysis and Reduction of Parasitic Effects in Induction Motors With Die-Cast Rotors

ALEXANDER STENING

Doctoral Thesis
Stockholm, Sweden 2013

KTH
Electrical Energy Conversion
School of Electrical Engineering
SE-100 44 Stockholm
SWEDEN

TRITA-EE 2013:011
ISSN 1653-5146
ISBN 978-91-7501-682-5

Akademisk avhandling som med tillstånd av Kungl Tekniska högskolan framlägges till offentlig granskning för avläggande av teknologie doktorsexamen torsdagen den 4 april 2013 klockan 14.00 i F3, Kungl Tekniska högskolan, Lindstedtsvägen 26, Stockholm.

Tryck: Universitetsservice US AB

Abstract

This thesis presents a study of inter-bar current effects on induction motors with die-cast aluminium and die-cast copper rotors. The parasitic effects introduced by these currents are analyzed and possible solutions to these problems are presented. This is realized by developing analytical tools for the simulation of inter-bar current effects. The methods used are verified by measurements on prototype machines. It is shown that the inter-bar currents can have a considerable effect on the motor starting performance, which can result in a reduced pull-out torque. At rated operation, this is seen as increased harmonic rotor currents, having a negative effect on the motor performance.

Results from calorimetric measurements show, that the efficiency gained when substituting a skewed die-cast aluminium rotor with a skewed die-cast copper rotor, is less than the theoretical expectation. It is shown that this is a result of a reduced power factor for the copper rotor. High inter-bar currents are believed to be the origin of this effect, increasing the harmonic content in the rotor magnetomotive force. This would be seen as an increased rotor leakage reactance. Results from locked-rotor tests, and simulations using measured values of inter-bar resistance, support this theory.

It is shown, that these negative effects are suppressed to a negligible level by the use of an unskewed rotor, but to the expense of a large synchronous torque at a low speed. By using a modulated rotor concept, having an asymmetrical rotor slot distribution, an unskewed rotor is designed to reduce this parasitic torque. Measurements on a prototype machine show that the modulated rotor suppresses both the inter-bar currents and the synchronous torque, resulting in an improved starting performance, without any significant change of the motor efficiency. The presented results strengthen the potential of the modulated rotor concept, introducing new possibilities for the reduction of negative effects appearing in induction machines.

Keywords: Aluminium rotors, asynchronous torques, copper rotors, die-cast rotors, induction machines, inter-bar currents, modulated rotors, starting torque, stray losses, synchronous torques.

Sammanfattning

Denna avhandling presenterar en studie av tvärströmmar i induktionsmaskiner med pressgjutna aluminium- och kopparrotorer. De parasitiska effekter som introduceras av dessa strömmar analyseras och möjliga lösningar på dessa problem presenteras. Detta utföres genom att utveckla analytiska verktyg för simulering av tvärströmmar. De använda metoderna verifieras genom mätningar på prototypmaskiner. Det visas att tvärströmmar påverkar induktionsmaskinens startegenskaper kraftigt vilket kan leda till ett reducerat kippmoment. Vid märkdrift ses ett ökat övertonsinnehåll i rotorstavströmmarna vilket har en negativ inverkan på maskinens prestanda.

Baserat på kalorimetriska mätningar visas att verkningsgradsökningen som erhålles då en sneddad aluminiumrotor ersättes av en sneddad kopparrotor är mindre än den teoretiska förväntningen. Orsaken till detta visas vara att effektfaktorn är lägre för kopparrotorn än för aluminiumrotorn. Denna skillnad kan vara orsakad av höga tvärströmmar i kopparrotorn vilka ökar övertonsinnehållet i den av rotorstavströmmen alstrade magnetomotoriska kraften, vilket således ses som en ökad läckinduktans på rotorsidan. Resultat från motorprov med låst rotor samt simuleringar med uppmätta värden av kontaktresistans styrker denna teori.

Det visas att dessa negativa effekter reduceras till en försumbar nivå genom att använda en rotor utan spårsneddning, men med nackdelen att ett kraftigt synkront moment uppstår vid en låg hastighet. Genom att använda ett modulerat rotorkoncept med en asymmetrisk spårfördelning utvecklas en rotor för att reducera detta parasitiska moment. Mätningar på en prototypmotor visar att denna rotor reducerar både tvärströmmar och det synkrona momentet, vilket resulterar i förbättrade startegenskaper utan någon signifikant förändring av verkningsgraden. De resultat som presenteras visar tydligt potentialen av det modulerade rotorkonceptet, vilket ger nya möjligheter för att motverka negativa effekter i induktionsmaskinen.

Sökord: Aluminiumrotorer, asymmetriska rotorspår, asynkronmaskiner, asynkrona moment, kopparrotorer, pressgjutna rotorer, startmoment, synkrona moment, tillsatsförluster, tvärströmmar.

Acknowledgements

This work was carried out within the High Performance Electrical Machines and Drives Program of the Center of Excellence in Electric power Engineering at the department of Electrical Energy Conversion, Royal Institute of Technology, in Stockholm, Sweden.

First of all, I would like to thank my supervisor Professor Chandur Sadarangani for guiding me throughout this project and for sharing his great experience in our conversations. I would also like to thank Associate Professor Juliette Soulard for always believing in me and for inspiring me whenever I needed it. I would like to thank the personnel at ABB LV Motors and ITT Flygt for giving me rewarding stays outside KTH, and for the cooperation throughout this project. A special thanks goes to Jörgen Engström and Bo Malmros, for their useful inputs and for supplying the first prototype motors, providing a good start to this project. Thanks to Tanja Hedberg for supplying equipment to the calorimetric test setup. Furthermore, I would like to thank Per-Åke Sahlin for helping me with the final prototype machines, and Freddy Gyllensten for giving me the time I needed to finish this thesis.

Throughout this project I have received at lot of help from the personnel of the Electrical Machines Laboratory, special thanks goes to Jan Timmerman, Stephan Meier, Alia Cosic, and the technicians Olle Brännvall and Jesper Freiberg. I am also very grateful to Eva Pettersson, Emma Geira and Celie Geira for helping me with administration, and to Peter Lönn for solving my computer problems.

During my time at KTH I have made a lot of friends with whom I have shared great moments, I am truly grateful to you all. Thanks to all former colleagues at EME and all present colleagues at E2C for contributing to the EME-spirit and for participating in various kinds of Roebel-activities, making my PhD-studies a rememberable time.

Finally, I would like to thank my family for their continuous support and for always helping me in every way. Last, but definitely not least, I wish to express my deepest gratitude to Ida Axelsson for her endless love and understanding.

Alexander Stening
Stockholm, February 2013

Contents

Chapter 1

Introduction

1.1 Background

In order to reduce the consumption of energy, it is important to reduce the losses created in the conversion between mechanical and electrical energy, and vice versa. Electrical machines are widely used for this conversion, in particular the induction machine, being the most commonly used electrical machine. The manufacturing of high efficient induction machines is therefore a topic of great interest.

During the years, the induction machine designs have been refined, making the loss reduction quite challenging. This requires not only the minimization of the well known stator and rotor copper losses, iron losses and friction losses, but also the reduction of the additional losses. These losses are defined as the additional losses that occur in the machine over the normal losses that are considered in usual induction motor performance calculations. At rated load, the additional losses are referred to as stray-load losses. For small to medium sized induction motors these losses vary typically within the range 0,5% - 3% of the motor input power [1, 2]. Measurements have, however, shown that these losses can be even larger [2, 3].

Small to medium sized induction machines are usually manufactured with die-cast aluminium rotors. The die-cast rotor is a cost effective solution for mass production of induction machines. Furthermore, the current progress in casting technology has also enabled the manufacturing of die-cast copper rotors. The higher conductivity of copper reduces the rotor cage losses. In [4], Peters et al. present results from measurements on a large number of die-cast copper rotors ranging 3-19 kW, where the aluminium simply had been replaced by copper. The results showed rotor I^2R loss reductions of about 40%, giving a total loss reduction of 11-19%.

These rotors where manufactured without cooling fins on the short-circuit rings, but instead, a more efficient shaft mounted internal fan was used, also providing a substantial reduction of the friction and windage losses. Furthermore, if the machine is redesigned to utilize the full potential of the copper rotor, the overall loss reduction can be increased even further [5, 6, 7, 8].

Rotor skewing is a common practice to reduce the audible noise of the machine [9]. If the rotor bars are insulated, rotor skewing also suppresses the asynchronous torques during a direct-on-line start, and reduces the harmonic cage losses at rated operation [10]. However, the absence of slot insulation in skewed die-cast rotors introduces undesired effects, such as inter-bar currents. These currents, flowing between the rotor bars, increase the asynchronous torques during a direct-on-line start [11], and can increase the stray-load losses [12, 13]. The losses associated with these currents can stand for a large part of the stray-load losses [3].

Some of our industrial partners have experienced that the efficiency gained when substituting a die-cast aluminium rotor with a die-cast copper rotor, was less than the theoretical expectation. It was believed, that this was the effect of inter-bar currents. These currents are strongly influenced by the inter-bar resistance and it is reasonable to assume that this resistance depends on the cage material and the die-casting process. This suggests differences, in terms of inter-bar current effects, between the aluminium and the copper rotor concepts.

1.2 Main Objectives

The overall objective of this thesis is to evaluate the effects of inter-bar currents on die-cast aluminium and die-cast copper rotors. It is of particular interest to determine if, as indicated from the initial investigations, the given set of copper rotors are less efficient than expected theoretically. In that case, the reason for this should be determined. It is also the intention of this work to propose possible solutions to reduce some of the parasitic effects that deteriorate the machine performance.

The project can be separated into different parts, some of which also describe the methodology used to fulfill the objectives, as follows:

- Measure the inter-bar resistance on a set of aluminium and copper rotors.
- Develop a computer program for the calculation of inter-bar current effects in induction machines, also considering skin-effect and saturation of the leakage paths.

- Verify the analytical models by measurements of starting performance and losses at rated operation.
- Evaluate the results and highlight differences between copper and aluminium rotors, where the stray-load losses are of special interest.
- Propose a new machine design that will reduce the derating effects that have been found, and verify this theory by measurements on a prototype machine.

1.3 Outline of the Thesis

This thesis consists of two main parts. The first part aims at an evaluation of inter-bar current effects in symmetrical die-cast rotors, where the comparative analysis between aluminium and copper rotors is of particular interest. The second part of the thesis presents the prototype machine that was designed to reduce some of the negative effects observed on these rotors.

Chapter 1: Introduces the thesis, gives a brief introduction to the topic and presents the objectives and the main contributions.

Chapter 2: Presents the method used to determine the inter-bar resistivity and the analytical model used to evaluate inter-bar current effects on motor performance.

Chapter 3: Compares die-cast copper rotors and die-cast aluminium rotors, both theoretical and experimental results are presented.

Chapter 4: Introduces the modulated rotor concept. First, existing modulated designs are simulated and compared with symmetrical rotors. Secondly, a prototype rotor is designed for an improved performance, the results are verified by measurements.

Chapter 5: The last chapter concludes the thesis, the main findings are presented and suggestions for future work are given.

1.4 Main Scientific Contributions

The main contributions of this work are:

- Measurements have shown that the inter-bar resistivity in the studied die-cast copper rotors is at least ten times lower than in the studied die-cast aluminum rotors.
- The starting torques of one aluminium- and one copper rotor skewed by one stator slot pitch have been measured. The results show that the pull-out torque is lower for the copper rotor than for the equivalent aluminum rotor. This was verified by simulations.
- Calorimetric measurements have been performed on one aluminium- and one copper rotor skewed by one stator slot pitch. The results show that the loss reduction obtained for the copper rotor is lower than expected theoretically, this was due to a reduced power factor of the copper rotor.
- A new modulated rotor design has been simulated and compared with skewed and unskewed symmetrical rotors. The results were verified by measurements on prototype machines. It was shown that the proposed modulated rotor suppressed both inter-bar currents and synchronous torques, without any significant change of the motor efficiency.

1.5 List of Appended Publications

I. **A. Stening** and C. Sadarangani, "The effects of inter-bar currents in cast aluminium and cast copper rotors," in Proceedings of *International Conference on Electrical Machines (ICEM'08)*, Vilamoura, Portugal, Sep. 2008.

II. **A. Stening** and C. Sadarangani, "Starting performance of induction motors with cast aluminium and copper rotors including the effects of saturation and inter-bar currents," in Proceedings of *International Conference on Electrical Machines and Systems (ICEMS'09)*, Tokyo, Japan, Nov. 2009.

III. **A. Stening** and C. Sadarangani, "A Comparative Study of Parasitic Effects in Induction Motors With Die-Cast Copper and Die-Cast Aluminium Rotors," submitted for review to *IEEE Transactions on Energy Conversion*.

IV. **A. Stening**, B. Larsson and C. Sadarangani, "Measurements of Stray Losses in Induction Machines With Die-Cast Aluminium Rotors," in Proceedings of *International Conference on Electrical Machines and Systems (ICEMS'12)*, Sapporo, Japan, Oct. 2012, selected for review to *IEEE Transactions on Industrial Applications*.

V. **A. Stening** and C. Sadarangani, "Performance Analysis of Asymmetrical Rotor Induction Motors," in Proceedings of *Portuguese-Spanish Conference on Electrical Engineering (XIICLEEE'11)*, Ponta Delgada, Azores, Jun.-Jul. 2011.

VI. **A. Stening** and C. Sadarangani, "Reduction of Synchronous Torques in Induction Machines Using Asymmetrical Rotor Slots," in Proceedings of *International Conference on Electrical Machines and Systems (ICEMS'12)*, Sapporo, Japan, Oct. 2012.

VII. **A. Stening**, U. Shaukat and C. Sadarangani, "New Design Options For Induction Machines Using Modulated Rotor Slots," submitted for review to *IEEE Transactions on Energy Conversion.*

1.6 Related Publications

- A. Krings, S. Nategh, **A. Stening**, H. Grop, O. Wallmark and J. Soulard, "Measurement and Modeling of Iron Losses in Electrical Machines," in Proceedings of *International Conference Magnetism and Metallurgy (WMM'12)*, Ghent, Belgium, Jun. 2012.

1.7 The Investigated Machines

Two different induction machines have been used for the experimental verifications. One 11 kW machine was subject for the evaluation of the die-cast copper rotor concept, and one 15 kW machine was used to evaluate the performance of the modulated rotor concept.

1.7.1 The 11 kW Machine

For the comparison of aluminium and copper rotors, a totally enclosed 4-pole 11 kW induction machine with a shaft height of 132 mm was used. One single stator, having 36 slots and a full pitch single layer winding, was used for all the measurements. The punched rotor laminations, having the same geometry and quality, were machined after the casting process to obtain the same diameters. The analysis of this machine is limited to the three different rotor concepts presented in Table 1.1. The slot shapes of all these rotors are semi-closed, according to Fig. 1.1.

The short-circuit rings of the copper rotor had less volume than in the aluminium case, and were lacking cooling fins. Therefore, the short-circuit rings of the skewed aluminium rotor were machined down, obtaining exactly the same geometry as for the copper rotor. Furthermore, high efficient bearings were used in order to reduce the influence of the frictional torque on the machine tests.

Rotor concept	Slot distribution	Number of slots	Cage material	Rotor skew
A1	Symmetrical	28	Cu	1 stator slot pitch
A2	Symmetrical	28	Al	1 stator slot pitch
A3	Symmetrical	28	Al	No skew

Table 1.1: Die-cast rotors tested for the 11 kW machine.

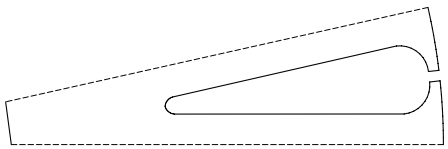

Figure 1.1: Slot shape for the rotors used in the 11 kW machine.

1.7.2 The 15 kW Machine

In the second part of the thesis, a standard 4-pole 15 kW induction motor with a shaft height of 160 mm is studied. The stator of this machine had 36 slots and a full pitch single layer winding. All the investigated rotors presented in Table 1.2, were designed with closed slots according to Fig. 1.2, and were tested in the same stator. The rotors were manufactured with the same quality of electrical steel. The iron laminations of the symmetrical rotors were punched, whilst the iron laminations of the modulated rotor were laser-cut. All rotors were machined after the casting process to obtain the same dimensions.

Rotor concept	Slot distribution	Number of slots	Cage material	Rotor skew
B1	Symmetrical	28	Al	30/36 stator slot pitch
B2	Symmetrical	28	Al	No skew
B3	Asymmetrical	28	Al	No skew

Table 1.2: Die-cast rotors tested for the 15 kW machine.

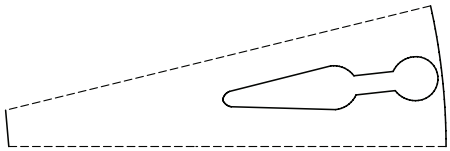

Figure 1.2: Slot shape for the rotors used in the 15 kW machine.

Chapter 2

Method for the Analysis of Inter-Bar Currents

Measurements of inter-bar resistance and analytical modeling of inter-bar currents have been important parts of this work. Section 2.1 introduces the method used in **Publication I** for the measurements of inter-bar resistance, experienced problems are discussed and possible solutions are presented. Section 2.2 briefly introduces the model used in the appended papers to account for inter-bar currents. This section also presents the additional effects considered during a direct-on-line start, relevant to **Publication I**, **II**, **V** and **VII**. In Section 2.3 the effects of inter-bar currents on motor performance are discussed, an example from **Publication VII** is presented, highlighting the parasitic effects introduced by these currents.

2.1 Measurements of Inter-Bar Resistance

The casting process results in a low resistive path between the rotor cage and the iron core. The resistance between two adjacent rotor bars, excluding the short-circuit rings, is referred to as inter-bar resistance. This resistance is usually converted to inter-bar resistivity by multiplying with the stack length. It is not possible to measure the inter-bar resistivity directly, it has to be calculated from measurements.

2.1.1 Method

In 1958, Odok presented a method to measure inter-bar resistance on casted rotors [14]. A direct current is fed into one short-circuit ring and taken out through the shaft on the opposite side. The voltage drop between the ring and the iron core is measured along the axial direction. Based on the average value of this voltage, the

inter-bar resistivity is calculated. Odok came to the important conclusion that the inter-bar impedance can be assumed to be purely resistive. This method was further developed, among others by Dabala in [15], also considering the distribution of the bar currents by assuming an equally distributed inter-bar resistivity. However, when die-cast copper rotors were introduced, these measurements became even more challenging. Dabala suggested an improved method for measurements on casted copper rotors [16]. This improved method, also considering the resistivity of the iron sheets, was used for the determination of the inter-bar resistivity in this project.

2.1.2 Test Setup

A test-rig was developed, shown in Fig. 2.1, making it possible to measure the inter-bar resistance with a negligible impact on the rotor construction. The top of the rig, on which the rotor is standing, consist of a smooth aluminium plate. One end of the rotor shaft was insulated with a thin plastic film and inserted into a hole in the center of this plate, creating a conducting path between the plate and the short-circuit ring. In order to create a uniform distribution of the current in this contact path, the aluminium plate was machined as well as the surface of the short-circuit ring. To complete the current path a copper ring is mounted on the other side of the shaft. With a potential difference between this copper ring and the aluminium plate, a current flows from one short-circuit ring to the shaft on the opposite side via the bar to core region. The inter-bar resistivity was calculated from measurements of the ring-to-ring voltage U_{AB} and the ring-to-shaft voltages U_{AD} and U_{BC}, using the equivalent rotor circuit proposed by Dabala. See Fig. 2.1(a) to identify positions A, B, C and D.

It is, however, appropriate to note some important issues regarding these measurements. As this setup basically is a short-circuit, it requires a relatively high current in order to obtain measurable voltage levels (at least 100 A for the tested rotors). It is also of great importance to exclude the connection points of the rotor to the test-rig from the voltage measuring circuit. It turned out, during the development of this test-rig, that the currents where not evenly distributed between the rotor bars. Especially for the copper rotors which where incidently manufactured without any cooling fins on the short-circuit rings. One reason for the uneven distribution is of course that the inter-bar resistivity might be unevenly distributed. An improvement was obtained by placing a conducting washer between the aluminium plate and the rotor short-circuit ring, according to Figure 2.1(c). This washer, being quite soft, distributes the force more equally around the short-circuit ring, resulting in a smoother distribution of the current in this contact region.

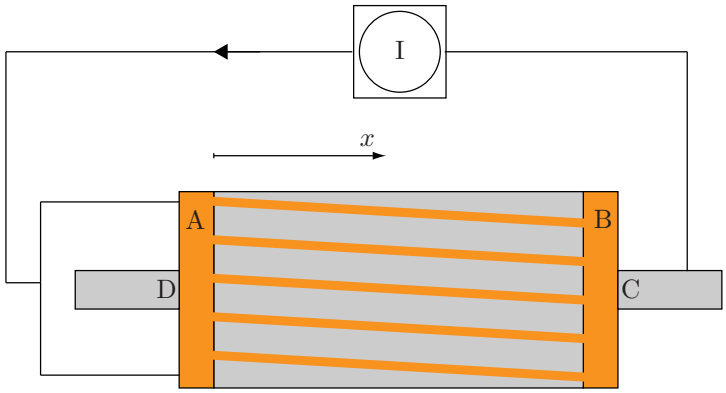

(a) Circuit.

(b) Rotor test-rig.

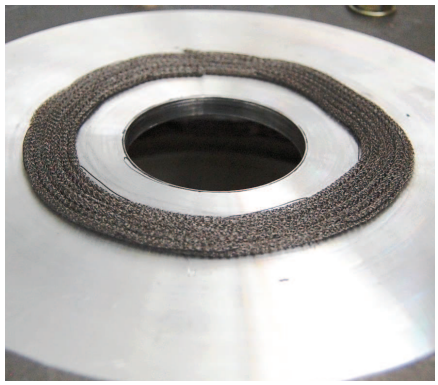

(c) Conducting washer between test-plate and rotor.

Figure 2.1: Rotor test setup for measurements of inter-bar resistance.

2.2 Inter-Bar Current Model

The analytical model used to include the effects of inter-bar currents is derived from Behdashti´s work in [17, 11]. These currents are taken into account by introducing a transverse bar to bar resistivity distributed along the rotor bars. Based on Behdashti´s proposed equivalent circuit of the rotor, the inter-bar current distribution along the rotor core can be obtained. Harmonic effects are included by considering MMF space harmonics up to the order of the first stator slot harmonics, and the distortion of the airgap permeance due to the stator slotting is considered using the model presented in [17]. However, the following assumptions are made in the model to simplify the calculations:

- The stator and rotor iron is assumed to have infinite permeability.
- The rotor slotting do not contribute to the permeance variation along the airgap circumference.
- The winding currents are assumed to vary sinusoidally in time.

Apart from the machine geometry and the inter-bar resistivity, this model requires the fundamental stator current as an input parameter. For a more accurate result, some additional effects are therefore included to calculate the fundamental stator current:

- Saturation of the leakage paths is considered by introducing saturation factors derived from FEM-simulations of locked-rotor tests.
- The skin effect in the rotor bars is considered using the one dimensional numerical method derived in [18].
- Inter-bar current effects are also considered for the calculation of the fundamental current.

The methods used to include these effects are presented further in **Publication II**, it is also shown that this results in a more accurate estimation of the fundamental stator current during a direct-on-line start.

The harmonic rotor currents are calculated from the fundamental current, also considering the skin effect in the rotor bars. The procedure for the calculation of the motor performance for different slip s, harmonic order n, and inter-bar resistivity R_{tn} is shown in Fig. 2.2. A detailed description of this model is found in the Licentiate thesis by the author [19], where Behdashti´s model and the described modifications are derived.

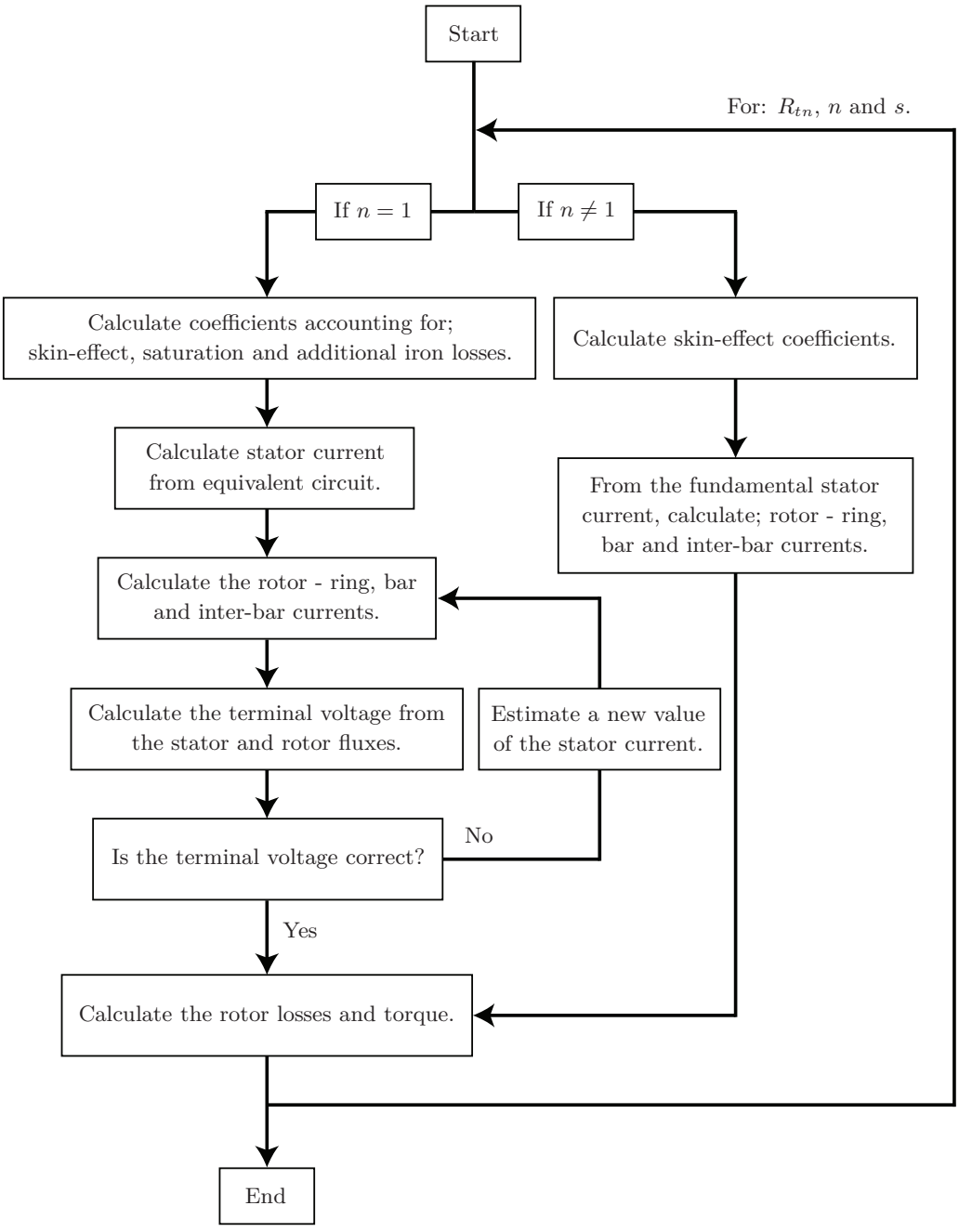

Figure 2.2: Procedure for the calculation of motor performance at different slip and inter-bar resistivity.

2.3 Effects of Inter-Bar Currents

All cage rotors have inter-bar currents unless the bars are perfectly insulated or, in case of an unskewed rotor, if the short-circuit ring impedance is zero [20]. However, with a normal short-circuit ring design, the inter-bar currents are usually negligible in the unskewed rotor [19]. The inter-bar currents are, therefore, mainly a problem in skewed rotors having a poor slot insulation. In these rotors, the airgap space harmonics having a wave length close to the rotor skewing angle, are particularly effective in inducing inter-bar currents. The inter-bar currents change the phase angle of the bar current along the bar length, in response to the induced electromotive force [21, 20], reducing the intended effect of rotor skewing. Besides increasing the harmonic torques during a direct-on-line start [11], inter-bar currents can increase the stray-load losses in the machine [12]. For mass produced machines the haphazard nature of the inter-bar resistivity also introduces additional differences between machines of the same type, resulting in a larger spread in performance with regard to starting torque and efficiency.

2.3.1 Example of the 15 kW Machine

In order to justify the studies in **Publication V** and **VII**, which investigate new rotor concepts to reduce the inter-bar currents, the negative effects of these currents were first simulated for the studied 15 kW machine equipped with a standard rotor. This section presents selected results from **Publication VII**, summarizing the results from the analytical model used in the study.

The torques during a direct-on-line start for a skewed and an unskewed rotor are shown in Fig. 2.3, for different levels of inter-bar resistivity, R_{tn}. The magnitudes of these resistivities are indicated in Fig. 2.4, showing the harmonic rotor cage losses at rated power.

In case of an unskewed rotor, the effects of inter-bar currents are negligible, and the absence of skew leakage increases the torque as compared to the skewed rotor. For the skewed rotor, bar insulation sufficiently reduces the inter-bar currents. As a result, the asynchronous torques created by the first order stator slot harmonics are sufficiently suppressed, and the high frequency cage losses at rated load are reduced. However, for a moderate value of the inter-bar resistivity, the inter-bar currents create large losses. The fundamental inter-bar currents increase the locked-rotor torque and the harmonic inter-bar currents increase the parasitic asynchronous torques created by the airgap space harmonics. These parasitic torques, counteracting the accelerating torque at higher speeds, reduce the pull-out torque of the machine. At rated load, this is seen as a substantial increase of the har-

monic rotor cage losses. In case of a low inter-bar resistivity, the magnitude of the asynchronous torques created by the inter-bar currents are similar to the unskewed case, and the corresponding harmonic cage losses are small.

From these results, it is obvious that only insulated rotor bars can utilize the full potential of rotor skewing.

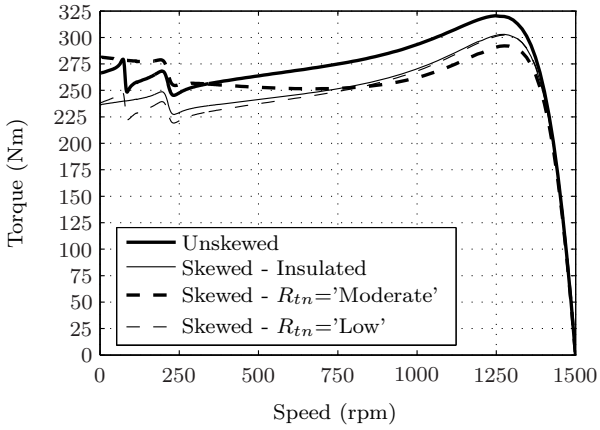

Figure 2.3: Starting torque for the 15 kW machine at different inter-bar resistivities R_{tn}.

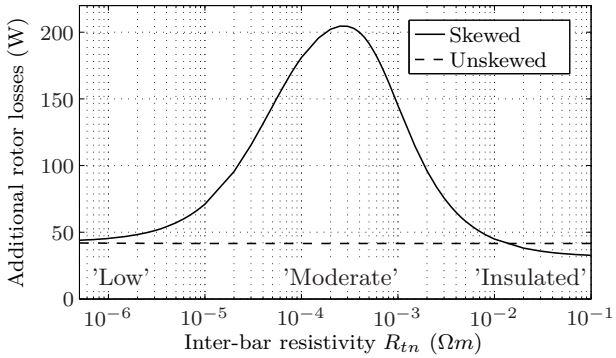

Figure 2.4: Additional rotor losses for the 15 kW machine at rated power as a function of inter-bar resistivity.

Chapter 3

Skewed Aluminium and Copper Rotors

This chapter summarizes the main findings from the study of the 11 kW machine equipped with aluminium and copper rotors. Section 3.1 presents the important results from the measurements of inter-bar resistance presented in **Publication I**. The starting performance is evaluated in Section 3.2, supplementing the results presented in **Publication I** and **II**. The expected differences in terms of inter-bar current losses between the two rotor concepts are evaluated in Section 3.3, and the measured motor performances are presented in Section 3.4, this summarizes the main findings in **Publication III**. Different methods to suppress inter-bar currents are discussed in Section 3.5. Experimental results, evaluating the effect of rotor skew on stray-load losses, which are presented in detail in **Publication IV** are also highlighted in this section.

3.1 Inter-Bar Resistivity

In **Publication I**, the inter-bar resistivity was calculated from measurements on a set of aluminium and copper rotors. The results obtained are shown in Table 3.1. The inter-bar resistivities of the copper rotors are of the same magnitude as those reported in [13]. The inter-bar resistivities of the aluminium rotors are very similar to those presented in [22], even though, in that work, the author removed

Rotor	Al 1	Al 2	Cu 1	Cu 2	Cu 3
R_{tn} [$\mu\Omega$m]	8,0	5,5	0,35	0,35	0,5

Table 3.1: Inter-bar resistivities R_{tn} calculated from measurements using a total rotor current of 200 A.

the short-circuit rings and measured directly between the rotor bars. From these results it can be concluded that the inter-bar resistivity is lower in the cast copper rotors than in the cast aluminium rotors. For the studied rotors, the difference is at least a factor of ten.

It was concluded, by investigating the voltage drop along the rotor bars, that the inter-bar resistivity could be unevenly distributed along the aluminium bars, whilst it seem more evenly distributed along the copper bars. These results are presented in detail in the Licentiate thesis by the author [19], and are consistent with the findings made by Dabala in [16].

3.2 Starting Performance

The torque speed characteristics for the two rotor concepts when starting direct-online was first investigated in **Publication I**, however, in that study the saturation of the leakage paths were unintentionally not included in the calculations. As a result, the calculated torques were underestimated at low rotor speeds. This mistake was corrected in **Publication II**, resulting in better correlations with the measured torques. It was discovered, unfortunately, that there was an error in the code for computing the effect of the first order stator slot harmonics. The harmonic torques presented in **Publication II** are therefore supplemented by this section, presenting the corrected simulations published in the Licentiate thesis [19]. These results were also calculated considering the slightly increased level of leakage path saturation for the copper rotor. It should be mentioned, that the main conclusions from the analysis in **Publication II** were not affected by this miscalculation.

Fig. 3.1(a) shows the torque speed characteristics in the case of insulated rotor bars for the two rotor concepts. In this case, the stator slot harmonics are sufficiently suppressed by the rotor skew. However, as the stator windings are not short-pitched the 5^{th} and the 7^{th} space harmonics, which have larger wave lengths than the slot harmonics and are therefore less affected by skewing, still cause asynchronous torques. As there are no inter-bar currents, the pull-out torques are expected to be the same for the two motor concepts. However, the copper motor is slightly more saturated in the leakage paths during a start, this results in a somewhat higher pull-out torque of the copper rotor.

Fig. 3.1(b) shows the simulation results using the measured values of inter-bar resistivity. Large asynchronous torques occur due to the first order slot harmonics, indicating large inter-bar current flow. It is believed, however, that the suitable combination of the slot numbers combined with the relatively large airgap reduces the influence the stator slot harmonics on the accelerating torque. The fundamen-

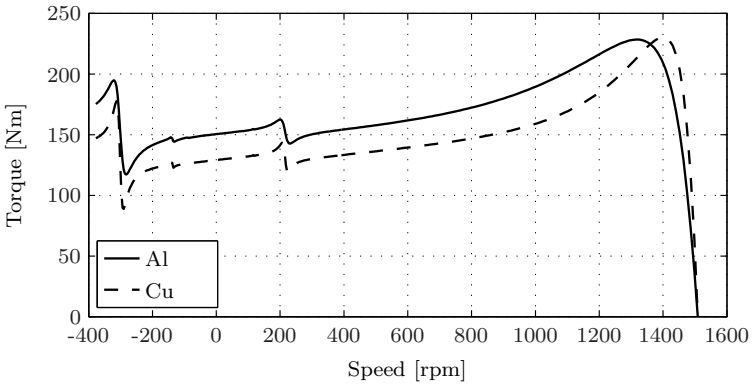

(a) Calculated for insulated rotor bars.

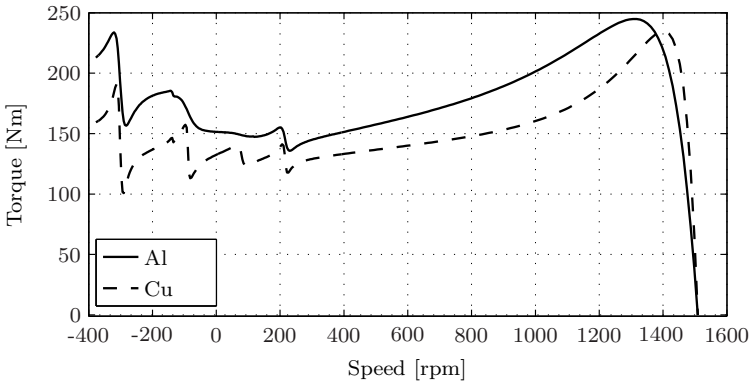

(b) Calculated for measured values of inter-bar resistivity.

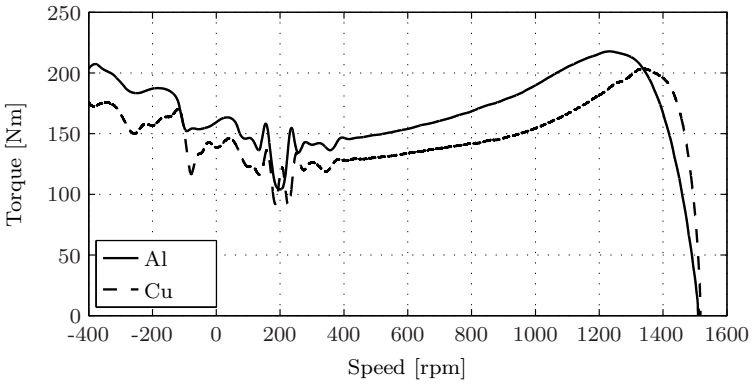

(c) Measured during a direct-on-line start.

Figure 3.1: Starting torque at rated voltage for the studied aluminium and copper rotors skewed by one stator slot pitch.

tal inter-bar currents are nevertheless increasing the pull-out torques for both rotor concepts. The pull-out torque is now 4,5 % higher for the aluminium rotor as compared to the copper rotor. This is a result of the higher inter-bar resistivity of the aluminium rotor.

The measurement results for the two rotors are shown in Fig. 3.1(c). First, the 4-pole motor was accelerated in reverse direction to 1000 rpm. Secondly, the torque was measured after shifting two phases of the sinusoidal supply voltage, forcing the machine to accelerate in the opposite direction. By doing this, the influence of the asynchronous torques could be measured with minimum distortion from the switching transient. The torque has been adjusted in quadratic relation to the voltage to account for the voltage drop during the start. Large asynchronous torques are created by the first order stator slot harmonics, and the pull-out torque is larger for the aluminium rotor. This verifies the prediction from the analytical model. The measured pull-out torque of the aluminium rotor is 7 % higher than the pull-out torque of the copper rotor. This is even larger than expected theoretically.

The measurements clearly show the presence of a synchronous torque at 214 rpm, however, its influence is suppressed by the rotor skewing. It should be mentioned that, since the simulations are based on a static model, it is difficult to model rapid changes in the rotor acceleration. This is probably the reason for the overestimated pull-out torques. However, the intention of this study was to compare the two concepts to distinguish differences in inter-bar current effects. It can be concluded that the lower inter-bar resistivity of the copper rotor results in a lower pull-out torque, as compared to the aluminium rotor.

3.3 Additional Rotor Losses

The relatively large difference between the inter-bar resistivities of the two rotors suggests different stray-load losses in the two rotor circuits. This theory is investigated in **Publication III**, where a comparative analysis between an aluminium rotor and a copper rotor is performed. The additional rotor losses simulated for the two rotors at rated power are shown in Fig. 3.2 as a function of the inter-bar resistivity. The arrows indicate the inter-bar resistivities calculated from measurements for the two studied rotors. Both of these figures are located on the left side of the theoretical loss peak in Fig. 3.2, hence, the losses are expected to increase with increasing inter-bar resistivity.

The measurements of the inter-bar resistances were performed at a rotor temperature of around 20 °C. In [23], Dorrell et al. found that the inter-bar resistance of an aluminium rotor increased by 410%, when the rotor was heated from 25 °C to

120 °C. Assuming a similar increase for the aluminium rotor being subject for this study, operating at 135 °C, additional rotor losses close to the theoretical maximum in Fig. 3.2 could be expected. If the same temperature coefficient applies for the copper rotor, operating at 117 °C, its inter-bar resistivity would still remain within the low loss region. This suggests a relatively large difference, in terms of inter-bar current losses, between the two studied rotors.

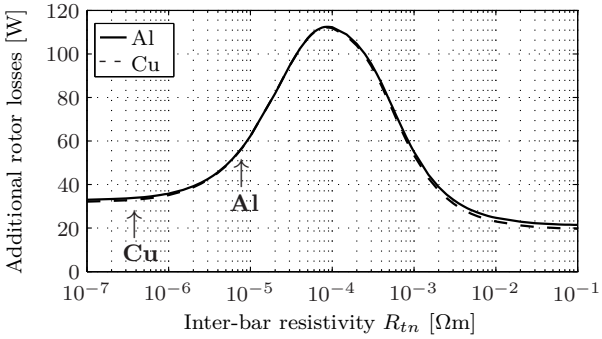

Figure 3.2: Additional rotor cage losses simulated as a function of inter-bar resistivity for the skewed rotors at the rated shaft power of 11 kW.

3.4 Rated and Partial-Load Test

Accurate measurement techniques are required to evaluate differences between the two rotor concepts, in particular as the stray-load losses are of special interest. It has been shown that, without doubt, the calorimetric approach can yield a more accurate loss measure than the more frequently used input-output methods, which, in turn, provides increased accuracy in the determination of the stray-load losses [24, 25, 26]. Therefore, a calorimetric test setup was developed for comparative measurements of different rotors in the same stator. From the calorimetric losses, the different loss components were calculated according to the present IEC-standard [27]. This section summarizes the main findings from the measurement results reported in **Publication III**.

The calorimetric measurements were performed with the intention to have the same test conditions for the two different rotors. The temperature of the stator housing was controlled by a water cooling system, also used for measuring the calorimetric power. The setup was calibrated to evaluate and to compensate for the power leakage (the heat not absorbed by the coolant). The construction and

the calibration of this calorimetric setup is described further in **Publication III**.

The main parameters determining the conditions and the repeatability of these measurements are described below; The average coolant temperature, T_{avg}, defined as the average value of the motor coolant input and output temperature, the ambient temperature, T_{amb}, surrounding the thermally insulated machine and the coolant flow, Q. In Table 3.2, showing the obtained calorimetric results at different output powers P_2, it can be seen that these parameters are controlled with an acceptable accuracy to obtain similar test conditions for each load point. These results strengthen the findings in the analysis that follow from these measurements.

Load	Rotor	T_{amb} (°C)	T_{avg} (°C)	ΔT (K)	Q (kg/min)	P_2 (kW)
25%	Al	21.7	21.5	2.879	3.275	2.53
	Cu	21.5	21.4	2.865	3.290	2.70
50%	Al	21.7	21.6	2.977	3.775	5.36
	Cu	21.5	22.0	3.042	3.745	5.36
75%	Al	21.7	21.6	3.110	4.785	8.12
	Cu	21.1	21.5	3.029	4.790	8.09
100%	Al	21.6	21.6	3.956	5.375	10.83
	Cu	21.4	21.4	3.785	5.315	10.88
110%	Al	21.6	21.7	4.703	5.385	12.04
	Cu	21.5	21.5	4.430	5.335	12.11

Table 3.2: Calorimetric results for the two different rotors mounted in the same 11 kW stator.

3.4.1 Stray-Load Losses

The stray-load losses are defined from the residual losses obtained for each load point. The residual losses, P_{Lr}, are defined from the total losses P_{Loss} as:

$$P_{Lr} = P_{Loss} - P_S - P_R - P_{Fe} - P_{fw} \tag{3.1}$$

Where P_S is the stator winding losses, P_R is the rotor winding losses, P_{Fe} is the iron losses and P_{fw} is the friction and windage losses. The residual losses, however,

contains information regarding the accuracy of the measurements, and can be used to identify possible sources of errors. These losses are shown in Fig. 3.3 as a function of normalized torque squared. The correlation coefficients obtained from the linear regression analysis of these residual losses are, for both the tested rotors, larger than 0.99. These figures exceed the lowest acceptable limit of 0.95, as defined by the standard [27], and imply a very accurate measuring technique. Furthermore, the intersections of the linear curves with the power axis are; 15 W and 12 W, for the aluminium rotor and the copper rotor, respectively. These intersections, being close to zero, imply a correct separation of the no-load losses. The obtained results clearly show the advantage of a direct loss measurement method.

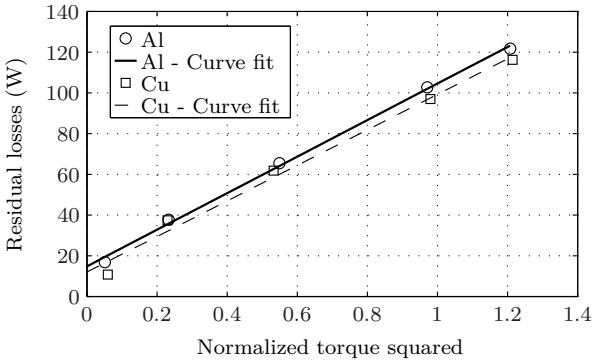

Figure 3.3: Residual losses as a function of normalized torque squared.

The stray-load losses at rated load, defined from the slopes of the two linear curves in Fig. 3.3, became 90 W for the aluminium rotor and 87 W for the copper rotor. The stray-load losses are, in this case, more or less unchanged when the die-cast aluminium rotor is replaced by the die-cast copper rotor. As lower inter-bar current losses were expected for the copper rotor, the results therefore suggest that the stray-load losses in this machine are redistributed, rather than reduced.

3.4.2 Efficiency and Power Factor

The lower bar resistivity of the copper rotor reduces the rotor cage losses, hence, an efficiency improvement is expected for all the load points, with the largest loss reduction occurring at high loads. The impact on the power factor is, in theory, negligible when aluminium is substituted by copper, provided that there are no inter-bar currents. However, based on the measured efficiency of the two studied machines shown in Fig. 3.4(a), the fundamental theory of loss reduction does not hold for all the load points. This is a result of a lower power factor for the copper

rotor, as shown in Fig. 3.4(b), increasing the load dependent losses. The main reason for this effect, introduced increasingly with the load, is believed to be a higher leakage inductance of the copper rotor.

From locked rotor tests it was concluded that the rotor leakage inductance, calculated at rated slip frequency, was almost 7% larger for the copper rotor compared to the aluminium rotor. A possible explanation could be the very low inter-bar resistivity of the copper rotor, resulting in high harmonic rotor currents, increasing the harmonic content in the rotor MMF. This would be seen as an increased leakage inductance. At rated speed, this effect is probably enhanced by the rotating permeance harmonics, increasing the difference between the two leakage inductances.

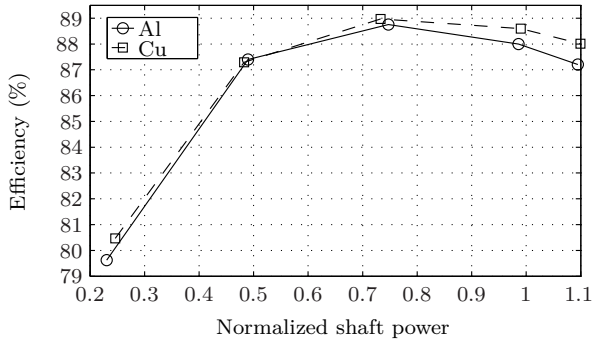

(a) Efficiency.

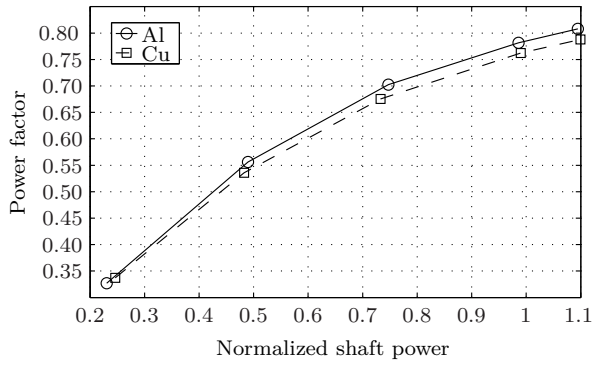

(b) Power factor.

Figure 3.4: Efficiency (a) and power factor (b) as a function of normalized shaft power.

3.4.3 Rated Performance

For a comparative analysis, the measured quantities at the load point corresponding to 100% load were corrected to exactly the rated power of 11 kW. The procedure for this is defined in the Appendix of **Publication III**. Table 3.3 shows the measured and the corrected values defining the ratings of the two studied machines. The power factor for the copper rotor is almost 3% lower than for the aluminium rotor, similar findings are presented in [4]. Reduced power factors for copper rotors have also been reported in [28], where a large number of machines have been tested, but it is not clear whether this was a result of a redesigned rotor slot or not. However, the reduced power factor measured for the copper rotor in this case increases the load dependent losses in the machine.

	Rotor	P_2 (kW)	U (V)	M (Nm)	n (rpm)	I (A)	$\cos(\phi)$ (-)	η (%)
Measured	Al	10.83	400	70.5	1468	22.78	0.782	87.9
	Cu	10.88	400	70.1	1483	23.28	0.762	88.6
Corrected	Al	11.00	400	71.6	1467	23.04	0.785	87.9
	Cu	11.00	400	70.8	1483	23.47	0.765	88.5

Table 3.3: Rated values for the 11 kW machine equipped with either a skewed copper rotor or a skewed aluminium rotor.

The efficiency gained when substituting aluminium with copper is 0.6 percentage. Considering only the fundamental component, and using the measured temperature rises of the stator winding and the rotor cage, the corresponding theoretical value is 1.1 percentage. Table 3.4 shows the separated loss components and the measured temperature rises for the two studied machines. The main differences are found in the stator and the rotor copper losses, as well as in the temperature rises of the two rotors. The stray-load losses are, in contrary to the expectations, not

Rotor	P_2 (kW)	P_S (W)	P_R (W)	P_{Fe} (W)	P_{LL} (W)	P_{FW} (W)	P_T (W)	T_{RS} (K)	T_{RR} (K)
Al	11.00	870	252	293	90	14	1519	74.2	115
Cu	11.00	904	129	289	87	17	1426	74.7	97

Table 3.4: Losses and temperature rises at rated power for the for the 11 kW machine equipped with either a skewed copper rotor or a skewed aluminium rotor.

lower in the copper rotor motor. However, the advantage of using copper instead of aluminium is obvious, but the lower power factor observed in this case reduces the expected efficiency gain.

3.5 Methods to Suppress Inter-Bar Currents

In this work, no attention is given to the winding design. A winding design producing less airgap space harmonics is, of course, one way to reduce the inter-bar currents. For mass produced induction machines, however, such a winding arrangement is more complicated and expensive to produce. A less expensive solution is to modify the die-cast rotor design, where the number of rotor slots and the rotor skew are crucial parameters for the reduction of inter-bar current effects [29].

For an optimized machine design the inter-bar currents can be reduced, but they can never be eliminated as long as the rotor bars are skewed, unless the bars are perfectly insulated.

3.5.1 Insulation Material in Rotor Slots

If insulation material is applied to the inner walls of the rotor slots prior to casting, the inter-bar resistance can be increased. The insulation material, however, must withstand high temperatures during the casting process. The melting points for aluminium and for copper are 660 °C and 1084 °C, respectively. This makes the insulation of die-cast copper rotors even more challenging. In [3], however, different inorganic insulation materials are proposed and tested, for example ceramic materials and phosphates. More recently, a large number of die-cast rotors having different grades of bar-to-iron insulation were tested [12], but the materials used are not given. Both these studies clearly show that the total losses can be reduced by insulating the rotor bars, resulting in a higher machine efficiency. It is of great importance, however, that the insulation procedure can be incorporated into the manufacturing process in an efficient way. The temperature requirement for the insulation material and the manufacturing aspects, are the main challenges for this solution.

3.5.2 Unskewed Rotors

An alternative solution is to remove the rotor skew, reducing the inter-bar currents to a negligible level, as long as the short-circuit ring impedance remains low. A removal of the rotor skew also reduces the flux leakage [10]. Thus, when starting direct-on-line an increased torque is obtained over the whole speed range, and at

rated operation an improved power factor can be expected.

In **Publication IV**, the 11 kW machine was used to evaluate the effect of rotor skew on motor losses. Two rotors were tested using the calorimetric method, one having a skew of one stator slot pitch, and the other rotor was unskewed. In contrary to what would be expected with the presence of inter-bar currents, the stray-load losses were reduced by approximately 10% for the skewed rotor. The absolute difference in stray-load loss, about 10 W, is small, and depends on the accuracy of the instrumentation used. However, one conclusion can still be made, the skewed rotor showed no significant change in the amount of stray-load loss compared to the unskewed rotor.

As the inter-bar currents are negligible in the unskewed rotor, some other source of stray-load loss increases for this machine. Previous research has shown [30], that the studied slot shape shown in Fig. 1.1 creates large eddy current losses in the open region towards the airgap. It is believed that these losses are increased when the rotor skew is removed. Furthermore, the studied 4-pole machine combined a 36 slot stator with a 28 slot rotor, this configuration is known to produce low inter-bar current losses. However, measurements on several rotors are required in order to draw any general conclusions regarding the effect of skewing on the total stray-load losses for this particular rotor design.

The removal of rotor skew is a simple and cost effective solution to reduce the inter-bar currents, however, there are some undesirable effects introduced instead. The increased coupling between the stator and the rotor will increase synchronous torques during a direct-on-line start. Depending on the load and the specific machine design, the machine might not accelerate up to rated speed, but instead, lock at stand-still or crawl at low speeds. Large synchronous torques can, for a given stator design, be avoided by choosing a suitable number of rotor slots [29, 10]. The rotor slot number is also one of the key parameters to avoid high audible noise levels [9], especially for unskewed machines. The choice of the rotor slot number, therefore, usually involves tradeoffs between different machine performances.

A possible solution to this problem is presented in [31], by introducing a modulated rotor concept combining different slot numbers into one single rotor, the rotor design is no longer limited to a certain slot number. Such a concept offers new opportunities to overcome negative effects created by a certain slot number, this solution is studied further in Chapter 4.

Chapter 4

Unskewed Modulated Rotors

This chapter presents an alternative method for the choice of the rotor slot number, also suppressing the inter-bar currents to a negligible level. By introducing the modulated rotor concept, combining different rotor slot numbers into one single unskewed rotor, the electromagnetic design is no longer restricted to a certain slot number. This flexible concepts offers possibilities to reduce negative effects appearing in unskewed symmetrical rotors, such as audible noise and synchronous torques. Section 4.1 introduces the different modulation techniques used in the appended publications. The starting performances and the losses at rated operation for two modulated rotors, designed for a reduced audible noise level [31], are simulated in **Publication V**. The main findings presented in this publication are summarized in Section 4.2. One of these designs is studied further in **Publication VI**, where synchronous torques are analyzed and modulation strategies reducing these torques are presented. The method used to suppress synchronous torques is introduced in Section 4.3, by presenting selected results from **Publication VI**. This method is used for the design of the modulated prototype rotor studied in **Publication VII**. This publication is summarized in Section 4.4 where the performance of this rotor is evaluated.

4.1 Modulation Strategies

Properties from different slot numbers can be combined by introducing an asymmetry in the rotor. The resulting harmonic spectrum of the rotor permeance contains properties from different rotor slot numbers. In the following, the total number of slots is referred to as primary slot number, and the additional slot numbers introduced by the modulation is referred to as inherent slot numbers. The asymmetry can, of course, be implemented in many different ways. In this section, two different

modulation methods are introduced.

4.1.1 Dual Rotor

In the Dual rotor concept [31], two different slot numbers are combined to form a rotor having a third number of rotor slots. The magnetic permeance of such a rotor is dominated by these three slot numbers, however, the influence of each slot number is reduced compared to the symmetrical case. In Fig. 4.1, one quarter of a Dual rotor combining the slot number 24 and 32 is shown, referred to as Dual 24:32. The total number of rotor slots is given by the average value of these two slot numbers, in this case 28. The Dual rotor concept is simple, but, it is limited to a certain number of combinations.

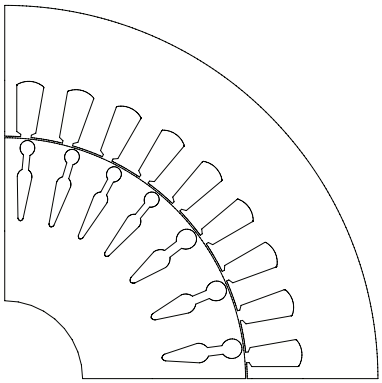

Figure 4.1: One quarter of a Dual 24:32 machine having 28 rotor slots and pole symmetry.

4.1.2 Progressive Sinusoidal Rotor

For a more flexible design, the Progressive Sinusoidal (PS) rotor provides an infinite number of combinations. For this concept, a certain modulation function is used to redefine the slot pitches and the slot widths of a symmetrical rotor. Starting with an initial symmetrical rotor design, having the slot width b_0 and the slot angle Θ_0, a PS modulated design is obtained by redefining the slot angle for slot number n_r as [31]:

$$\Theta(n_r) = \Theta_0(n_r) + \sum_{i=1}^{n} K_i \sin\left(i\Theta_0(n_r) + \delta_i\right) \tag{4.1}$$

Where K_i and δ_i are the modulation coefficients, determining the magnitude and the displacement of the modulation distribution, defined by the sine wave factor i.

In order to keep the flux densities in the rotor teeth unchanged, the slot width to teeth width is kept constant around the periphery. The corresponding rotor slot widths are, therefore, defined as

$$b(n_r) = b_0(n_r)\left(\frac{\Theta(n_r+1)-\Theta(n_r)}{\Theta_0(n_r+1)-\Theta_0(n_r)}\right). \tag{4.2}$$

Fig. 4.2 shows an example of a PS-rotor having 36 slots and pole symmetry, using $i = 4$ and $K_4 = 4$. Depending on the modulation coefficients used, new properties can be added to the rotor, reducing the influence of the primary slot number.

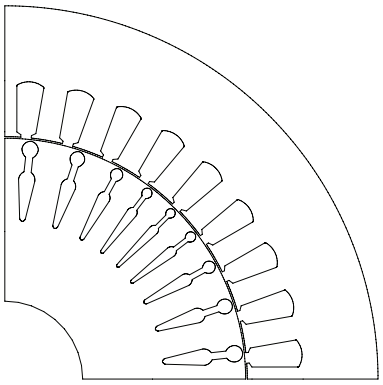

Figure 4.2: One quarter of a PS-rotor having 36 rotor slots and pole symmetry.

4.2 Evaluation of Existing Designs

When the rotor skew is removed, an increased audible noise level can be expected. In [31], however, it is shown that the radial airgap forces associated with high noise levels can be reduced by introducing a modulated rotor. Two of the designs suggested in that work, the Dual 24:32 rotor and one PS rotor, were studied further in [**Publication V**], with the intention to evaluate the starting performances and the losses at rated operation.

The results showed, based on FEM-simulations, that the stator and the rotor joule losses increased slightly for the modulated rotor compared to the unskewed symmetrical case. This is mainly due to increased harmonic cage losses. But the increase is small compared to the inter-bar current losses that can appear in the skewed rotor. From this investigation it can be concluded that the joule losses in the machine can be kept at a reasonable level, even though a rotor asymmetry is introduced.

It was observed, however, that the studied designs had problems with large synchronous torques at zero speed. In **Publication VI**, it is shown that this makes the Dual 24:32 rotor unsuitable for direct-on-line applications, since the rotor position at standstill determines whether the machine starts or not. It is also shown, that one of the inherent slot numbers for the Dual 24:32 rotor is 36, creating this negative effect. However, the low noise designs having problems to start direct-on-line can instead be promising concepts for inverter-fed operation.

4.3 Reduction of Synchronous Torques

The possibility to control the influence of different slot numbers can be used to suppress other parasitic effects appearing in symmetrical rotors. In **Publication VI**, a PS-modulation is used to suppress synchronous torques in unskewed rotors during direct-on-line starts. In one of the examples presented, as a worse case study, a 36 slot rotor is chosen for the 36 slot stator. In this case, the stator and the rotor slot space harmonics, created by the fundamental current, have the same number of poles. These waves rotates synchronously at zero speed, hence, a large synchronous torque is created. As a result, this machine will not accelerate up to rated speed when starting direct-on-line, but instead lock at standstill. By adding a PS-modulation to this rotor, the influence of the primary slot number can be reduced, hence, the corresponding synchronous torque is suppressed.

It can be shown, that the slot number 36 is efficiently suppressed by using the sine wave factor $i = 4$ in the PS-modulation, defined by Eq. 4.1. The Fourier analysis of the rotor permeance, normalized with respect to the symmetrical case, is shown in Fig. 4.3, using $i = 4$ and $k_4 = 4$. This result shows that the primary slot number is sufficiently suppressed for this modulation.

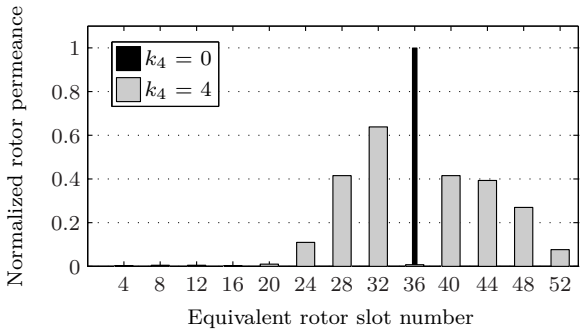

Figure 4.3: Dominating slot numbers for the 36 slot rotor, without PS modulation (black) and with PS modulation (grey).

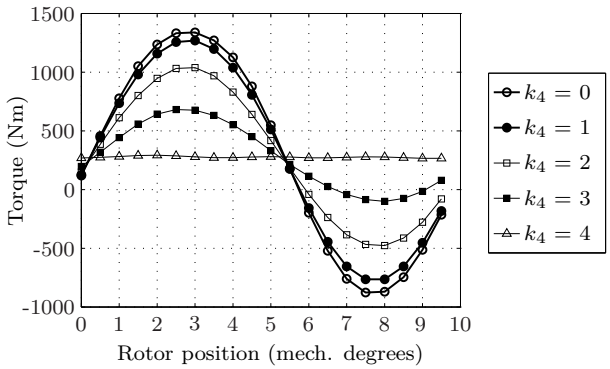

Figure 4.4: Locked rotor torque as a function of the rotor position for the 36 slot rotor at different levels of PS modulation.

Figure 4.4, shows the FEM-simulated locked rotor torque as a function of the rotor position, for different levels of modulation (different amplitudes of the factor K_4). This verifies the predictions from the Fourier analysis, and shows that the strong synchronous torque is almost eliminated for $K_4 = 4$. However, if the primary slot number has to be eliminated in the rotor permeance, one should not choose that number of slots in the first place. Nevertheless, this illustrates the potential of the modulated rotor concept, giving the possibility to adjust the influence of a specific slot number.

4.4 Prototype Machine

The standard rotor for the 15 kW machine had 28 slots and a skew of 30/36 stator slot pitch. When the rotor skew is removed, the synchronous torque at 214 rpm created by the interaction between the rotor slot harmonic of order 13 and the stator MMF harmonic of order 13, becomes quite large. For this stator design, this is a direct consequence of the rotor slot number. The prototype rotor was designed to suppress this torque by reducing the influence of the primary slot number. However, the slot number 28 has some desirable properties at rated operation. Therefore, it was not the intention to completely eliminate the primary slot number, but to reduce its influence and to introduce other suitable slot numbers instead. The manufactured prototype rotor was tested and compared with the corresponding skewed and unskewed symmetrical rotors, also providing information regarding the effect of skewing and inter-bar currents. This section summarizes the main findings present in **Publication VII**.

4.4.1 Design

The standard rotor geometry was used as a start for the design of the modulated rotor. By adding the PS modulation function according to (4.1), the slot widths and slot pitches were changed accordingly. After the design procedure it was verified that the prototype machine had exactly the same total slot area as the symmetrical standard design.

The sine wave factors, i, were chosen as a multiple of the pole number, in this case 4 and 8, maintaining the pole symmetry. Using the modulation coefficients $K_4 = 2.65$ and $K_8 = 2.2$, the inherent slot numbers 32 and 20 are introduced in the rotor permeance, according to Fig. 4.5. The resulting geometry for one quarter of the rotor is shown in Fig. 4.6. As the influence of the primary slot number 28 is reduced, a reduction of the synchronous torque at 214 rpm is expected. This is verified by the FEM-simulations in Fig. 4.7, showing the torque speed characteristics when starting direct-on-line. These results show that the synchronous torque is reduced by approximately 30% by using the proposed modulation. An improved starting performance can thereby be expected for the prototype rotor. In **Publication VII**, it is also shown that the torque ripple at rated operation is maintained at a reasonable level, as compared to the symmetrical case.

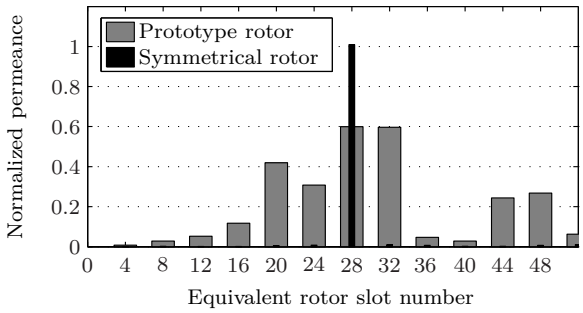

Figure 4.5: Dominating slot numbers included in the rotor permeance for the modulated prototype rotor.

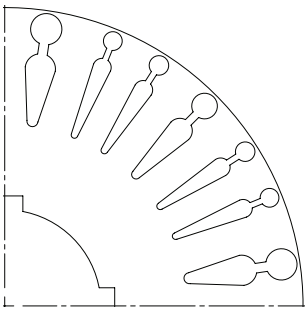

Figure 4.6: One quarter of the modulated prototype rotor, having pole symmetry.

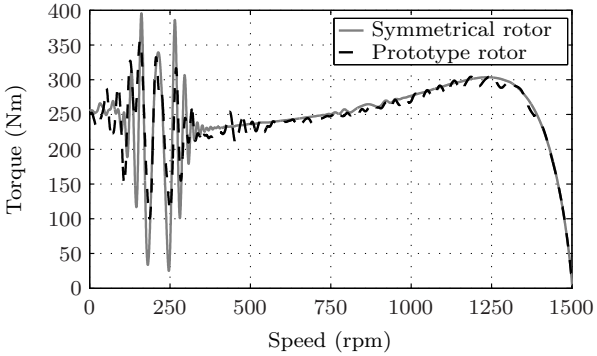

Figure 4.7: FEM-simulated starting torques for the two unskewed rotors.

4.4.2 Measurement Results

The torque-speed characteristics at rated voltage were measured continuously when the machine was decelerated from no-load to stand-still. The initial test setup used for measuring the variation of torque and current with speed was only adapted for measuring the fundamental component. However, additional measurements were performed in parallel, using a high sampling frequency, capturing the harmonic torques over time. As no calorimetric measurements could be performed on this machine, the total losses were defined as the difference between the input and the output power. The different loss components were then segregated according to the IEC-standard [27].

Starting Performance

The torques measured as a function of speed for the three different machines are shown in Fig. 4.8. For the skewed rotor, the increased locked rotor torque, and the reduced pull-out torque, are consistent with the predicted inter-bar current effects in Fig. 2.3. The measured pull-out torque of the skewed rotor is reduced by approximately 11% as compared to the unskewed rotors. According to the analytical results, the skew leakage only accounts for a torque reduction of about 5%. It is therefore believed, that a large part of the reduction can be attributed the braking torques created by the inter-bar currents in the skewed rotor.

To further investigate the impact of the synchronous torques, the torque recorded at a high sampling frequency is shown Fig. 4.9, when the machine was decelerated from no-load to stand-still. For the skewed rotor the synchronous torque introduced by the rotor slot number 28 is, of course, sufficiently suppressed. However, when comparing the unskewed rotors, this synchronous torque is reduced by approximately 30% for the modulated prototype rotor. This is consistent with the expectations from the corresponding FEM-simulations, as shown in Fig. 4.7. Hence, by removing the rotor skew, an improved starting performance can be achieved using a modulated rotor design.

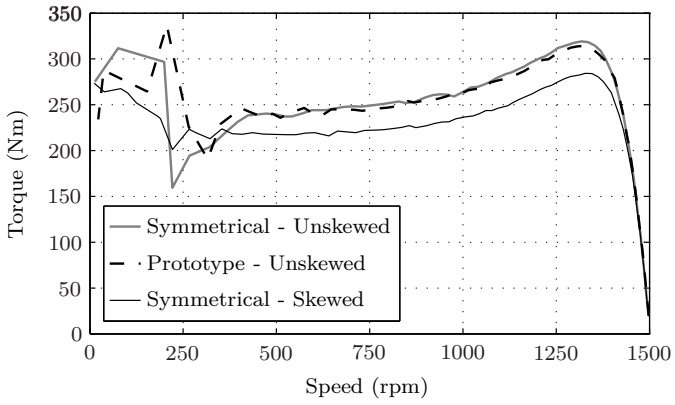

Figure 4.8: Measured torque as a function of speed for the different rotors tested in the same 15 kW stator.

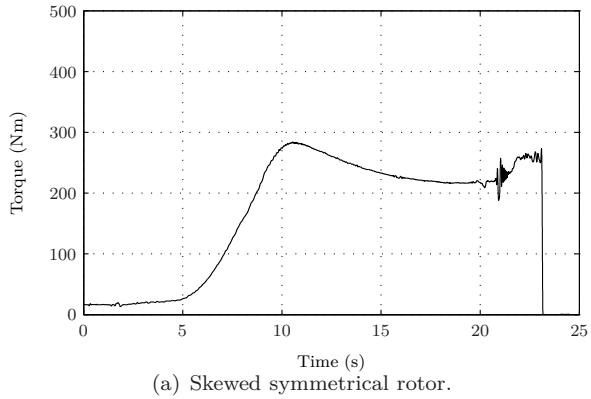

(a) Skewed symmetrical rotor.

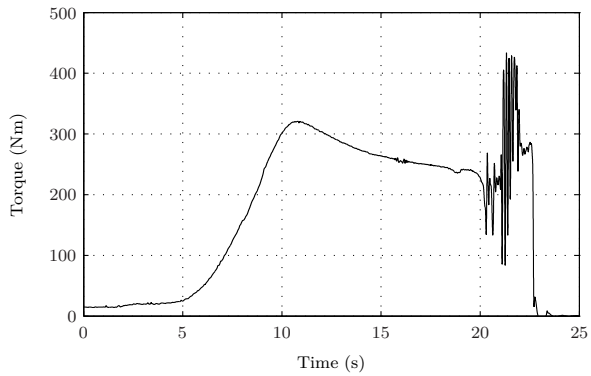

(b) Unskewed symmetrical rotor.

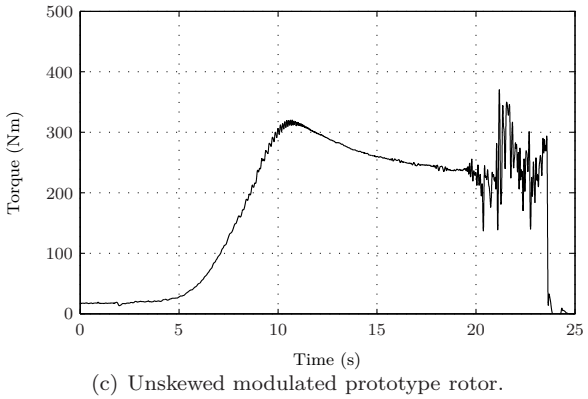

(c) Unskewed modulated prototype rotor.

Figure 4.9: Measured torque during deceleration from no-load to stand-still for the three rotors tested in the same stator.

Rated Operation

The question arises, of course, how the losses in the machine are affected by the asymmetry introduced. The results obtained for the three rotors, tested in the same stator, are summarized in Table 4.1. The main differences are found in the rotor losses and the iron losses. For these machines rotor skewing increases the iron-losses, this is consistent with the theory presented in [32]. The lowest iron-losses were observed for the modulated prototype rotor, a reduction of 10% compared to the skewed symmetrical rotor. However, the rotor losses increased for the modulated rotor design, giving approximately the same total losses as the skewed rotor. The stray-load losses, being hard to measure accurately with the method used, were in the same range for all three studied motors. This suggests that the stray-load losses were redistributed, rather than reduced, when the inter-bar current losses were suppressed by the removal of the rotor skew. However, it is the author's belief that a more accurate measuring technique is required for a comparison of skew effects on stray-load losses.

Based on these measurements it can be concluded that the asymmetry introduced by the modulated rotor did not result in a significant reduction of the rated efficiency. The modulated rotor has the same efficiency as the skewed symmetrical rotor. It shall be noted that there were some issues involved in the manufacturing of the modulated rotor. Unfortunately, as a result of the laser cutting of the iron sheets, the stacking factor was slightly reduced, resulting in aluminium leakage

Table 4.1: Measured quantities at the rated output power of 15 kW.

		Symmetrical Skewed	Symmetrical Unskewed	Prototype Unskewed
Stator winding temp.	(°C)	74.5	73.7	77.7
Stator winding losses	(W)	552	538	552
Rotor winding losses	(W)	297	277	303
Iron losses	(W)	343	325	308
Stray-load losses	(W)	284	309	293
Friction losses	(W)	76	69	88
Total losses	(W)	1552	1518	1544
Efficiency	(%)	90.7	90.9	90.7
Power factor	(-)	0.82	0.83	0.83
Line current	(A)	29.0	28.7	28.9
Speed	(rpm)	1471	1473	1471

during the casting process. Therefore, a deteriorated performance was expected for this rotor.

Chapter 5

Conclusions and Future Work

5.1 Conclusions

Measurements have shown that the inter-bar resistivity in the studied die-cast aluminium rotors is at least ten timer higher than in the equivalent die-cast copper rotors. Simulations of the skewed rotors have shown that this results in a higher pull-out torque for the aluminium rotor compared to the copper rotor, this was verified by measurements.

Calorimetric measurements showed, that the increase in efficiency obtained when substituting a skewed die-cast aluminium rotor with a skewed die-cast copper rotor having the same geometry, was less than the theoretical expectation. At the rated output power of 11 kW, the efficiency improvement was 0.6 percentage, the corresponding theoretical value is 1.1 percentage. The derating of the copper rotor was not a result of increased stray-load losses, but instead, an effect of a lower power factor. This could be a result of individual variations between the two studied rotors or measurement errors. But as similar results have been published by other researchers [4, 28], it is reasonable to believe that this is an effect created by the die-cast copper rotor as a concept. A possible explanation could be the very low inter-bar resistivity of the copper rotor, resulting in high harmonic rotor currents, increasing the harmonic content in the rotor MMF. This would be seen as an increased leakage inductance, reducing the power factor. Simulations and results from locked-rotor tests support this theory.

The effect of rotor skewing on a 15 kW induction machine with a die-cast aluminium rotor has been investigated. The measured pull-out torque was reduced by 11% when the rotor skew was introduced, simulations showed that the skew leakage only accounts for a torque reduction of 5%, a large part of the reduction can thereby

be attributed to the braking torques created by inter-bar currents. The unskewed rotor, having a slightly higher efficiency, experienced a large synchronous torque at a low speed, depending on the application this could result in an unsuccessful start.

To overcome these problems, an unskewed modulated rotor was designed, combining different slot numbers into one single rotor. By reducing the influence of the slot number creating the synchronous torque, an improved starting performance was expected, without eliminating the positive effects of this slot number at rated operation. This was analyzed using Fourier analysis of the rotor permeance and FEM-simulations verified these predictions.

Measurements on a prototype machine showed that the modulated rotor successfully reduces both the inter-bar currents and the synchronous torque, without any significant change of motor efficiency. This was achieved even though the casting of the prototype rotor incidently caused aluminium to leak between the iron sheets, reaching the surface of the rotor at some places, lowering the expectations of this rotor. These results confirm the potential of the modulated rotor concept as a flexible solution to reduce parasitic effects appearing in induction machines, and justifies further research on the concept to obtain refined machine designs.

5.2 Future Work

The theory suggesting that the inter-bar currents reduce the power factor of the copper rotor needs to be supported by repeated measurements, also considering other skewed copper rotors. The effect of rotor skewing on stray-load losses also needs to be evaluated for several rotors, it is of great importance to use accurate measuring techniques, the calorimetric method is recommended for this evaluation.

Different materials and methods to apply rotor slot insulation prior to casting is an important subject for further research. If such a procedure could be implemented in the industrial manufacturing process, one would expect less variations in motor performance between motors of the same type. Of course, as the rotor skew is fully utilized with insulated slots, increased motor efficiency could be obtained. For the copper rotors investigated in this thesis, having a very low inter-bar resistivity, slot insulation is also believed to increase the power factor of the motor.

The modulated rotor concept could be used to design rotors having a low content of harmonic currents in the rotor cage, suppressing the corresponding stray-load losses. However, it is the author's belief that such an analysis should consider the total losses in the machine. Minimizing only the harmonic rotor copper losses suggests less damping to the airgap space harmonics, which in turn, might result in increased harmonic iron losses. This evaluation could be performed by a parameterized FEM-model considering the total motor losses. However, it is important

to verify the starting performance for such a design, unless the motor is intended to be operated through an inverter.

The modulated rotors designed for a reduced audible noise in [31] could be promising concepts for inverter-fed operation, this should be investigated further by noise measurements on prototype machines.

Bibliography

[1] A.R. Hagen, A. Binder, M. Aoulkadi, T. Knopik, and K. Bradley. Comparison of measured and analytically calculated stray load losses in standard cage induction machines. *Proc. of International Conference on Electrical Machines*, pages 1–6, 2008.

[2] A.A. Jimoh, R.D. Findlay, and M. Poloujadoff. Stray losses in induction machines: Part i, definition, origin and measurement. *IEEE Trans. on Power Apparatus and Systems*, PAS-104:1500–1505, 1985.

[3] H. Nishizawa, K. Itomi, S. Hibino, and F. Ishibashi. Study on reliable reduction of stray load losses in three-phase induction motor for mass production. *IEEE Trans. on Energy Conversion*, EC-2:489–495, 1987.

[4] D. T. Peters, D. J. Van Son, J. G. Cowi, and E. F. Brush. Improved motor energy efficiency and performance through the die-cast copper rotor. In *Proc. of International Conference on Electrical Machines*, Aug. 2002.

[5] S. Lie and C. Di Pietro. Copper die-cast rotor efficiency improvement and economic consideration. *IEEE Trans. on Energy Conversion*, 10(3):419 –424, Sep 1995.

[6] R. Kimmich, M. Doppelbauer, D. T. Peters, J. G. Cowi, and E. F. Brush. Die-cast copper rotor motors via simple substitution and motor redesign for copper. In *Proc. of International Conference on Electrical Machines*, Sept. 2006.

[7] J. L. Kirtley, J. G. Cowie, E. F. Brush, D. T. Peters, and R. Kimmich. Improving induction motor efficiency with die-cast copper rotor cages. In *Proc. of IEEE PES General Meeting*, pages 1 –6, June 2007.

[8] D. T. Peters, E. F. Jr Brush, and J. L. Kirtley. Die-cast copper rotors as strategy for improving induction motor efficiency. In *Proc. of Electrical Insulation Conference and Electrical Manufacturing*, pages 322 –327, Oct. 2007.

[9] P. Vijayraghavan and R. Krishnan. Noise in electric machines: a review. *IEEE Trans. on Industry Applications*, 35(5):1007 –1013, sep/oct 1999.

[10] P. L. Alger. *Induction Machines: Their Behavior and Uses*. Taylor & Francis, 1995.

[11] A. Behdashti and M. Poloujadoff. A new method for the study of inter-bar currents in polyphase squirrel-cage induction motors. *IEEE Trans. on Power Apparatus and Systems*, PAS-98(3):902–911, 1979.

[12] Y.N. Feng, J. Apsley, S. Williamson, A.C. Smith, and D.M. Ionel. Reduced losses in die-cast machines with insulated rotors. *IEEE Trans. on Industry Applications*, 46(3):928 –936, May-June 2010.

[13] S. C. Englebretson. *Induction machine stray loss from inter-bar currents*. Ph.d. thesis, Massachusetts Institute of Technology, Sept. 2009.

[14] A. M. Odok. Stray-load losses and stray torques in induction machines. *AIEE Trans. on Power Apparatus and Systems*, 77(3):43–53, 1958.

[15] K. Dabala. A new experimental-computational method to determine rotor bar-iron resistance. *Proc. of International Conference on Electrical Machines*, 2:69–72, 1996.

[16] K. Dabala. Modified method to determine rotor bar-iron resistance in three-phase copper casted squirrel-cage induction motors. *Proc. of International Conference on Electrical Machines*, pages 231–234, 2006.

[17] A. Behdashti. *Contribution a l'etude des pertes supplementaires des machines asynchrones dans une tres large zone de fonctionnement*. PhD thesis, L'Institut national polytechnique de Grenoble, June 1975.

[18] C. Sadarangani. *Electrical machines - design and analysis of induction and permanent magnet motors*. KTH Hogskoletryckeriet, 2000.

[19] A. Stening. *On Inter-bar Currents in Induction Motors with Cast Aluminium and Cast Copper Rotors*. Licentiate thesis, Royal Institute of Technology (KTH), Stockholm, Sweden, June 2010.

[20] A. C. Smith, S. Williamson, and C. Y. Poh. Distribution of inter-bar currents in cage induction machines. In *Proc. of International Conference on Power Electronics Machines and Drives*, volume 1, pages 297 – 302, March 2004.

[21] S. Williamson and A. C. Smith. Equivalent circuits for cage induction motors with inter-bar currents. *Proc. of IEE Electric Power Applications*, 149(3):173 –183, May 2002.

[22] O. Aglén. *Calorimetric Measurements of Losses in Induction Motors.* Licentiate thesis, Royal Institute of Technology, Stockholm, Sweden, 1995.

[23] D.G. Dorrell, T.J.E. Miller, and C.B. Rasmussen. Inter-bar currents in induction machines. *IEEE Trans. on Industry Applications*, 39(3):677 – 684, may-june 2003.

[24] K. J. Bradley, Wenping Cao, and J. Arellano-Padilla. Evaluation of stray load loss in induction motors with a comparison of input-output and calorimetric methods. *IEEE Trans. on Energy Conversion*, 21(3):682 –689, Sept. 2006.

[25] Wenping Cao, K. J. Bradley, and A. Ferrah. Development of a high-precision calorimeter for measuring power loss in electrical machines. *IEEE Trans. on Instrumentation and Measurement*, 58(3):570 –577, March 2009.

[26] Wenping Cao. Comparison of IEEE 112 and new IEC standard 60034-2-1. *IEEE Trans. on Energy Conversion*, 24(3):802 –808, Sept. 2009.

[27] *Rotating Electrical Machines – Part 2-1: Standard Methods for Determining Losses and Efficiency From Tests (Excluding Machines for Traction Vehicles)*, IEC 60034-2-1: 2007 (BS EN 60034-2-1).

[28] D. Liang, X. Yang, J. Yu, and V. Zhou. Experience in china on the die-casting of copper rotors for induction motors. In *Proc. of International Conference on Electrical Machines*, Sep. 2012.

[29] B. Heller and V. Hamata. *Harmonic Field Effects in Induction Machines.* Elsevier Science Ltd, 1977.

[30] Ola Aglén. Calorimetric measurements of losses in air-cooled and water-cooled asynchronous motors. In *Proc. of International Conference on Electrical Machines*, volume 3, pages 256 –262, 1996.

[31] R. Chitroju. *Improved Performance Characteristics of Induction Machines with Non-Skewed Asymmetrical Rotor Slots.* Licentiate thesis, Royal Institute of Technology, Stockholm, Sweden, 2009.

[32] C.I. McClay and S. Williamson. The variation of cage motor losses with skew. *IEEE Trans. on Industry Applications*, 36(6):1563 – 1570, nov/dec 2000.

Appendix A

Publications

A.1 Publication I

A. Stening and C. Sadarangani, "The effects of inter-bar currents in cast aluminium and cast copper rotors," in Proceedings of *International Conference on Electrical Machines (ICEM'08)*, Vilamoura, Portugal, Sep. 2008.

Errata

On page 4:

The asynchronous torques of order 11 and 13 are now drastically increased in amplitude. Should read: The asynchronous torques of order 17 and 19 are now drastically increased in amplitude.

A.2 Publication II

A. Stening and C. Sadarangani, "Starting performance of induction motors with cast aluminium and copper rotors including the effects of saturation and inter-bar currents," in Proceedings of *International Conference on Electrical Machines and Systems (ICEMS'09)*, Tokyo, Japan, Nov. 2009.

Errata

Equation (8), should read: $I_1(s = s_p) = \frac{I_1(s=1)}{\sqrt{3}}$

A.3 Publication III

A. Stening and C. Sadarangani, "A Comparative Study of Parasitic Effects in Induction Motors With Die-Cast Copper and Die-Cast Aluminium Rotors," submitted for review to *IEEE Transactions on Energy Conversion*.

A.4 Publication IV

A. Stening, B. Larsson and C. Sadarangani, "Measurements of Stray Losses in Induction Machines With Die-Cast Aluminium Rotors," in Proceedings of *International Conference on Electrical Machines and Systems (ICEMS'12)*, Sapporo, Japan, Oct. 2012, selected for review to *IEEE Transactions on Industrial Applications*.

A.5 Publication V

A. Stening and C. Sadarangani, "Performance Analysis of Asymmetrical Rotor Induction Motors," in Proceedings of *Portuguese-Spanish Conference on Electrical Engineering (XIICLEEE'11)*, Ponta Delgada, Azores, Jun.-Jul. 2011.

A.6 Publication VI

A. Stening and C. Sadarangani, "Reduction of Synchronous Torques in Induction Machines Using Asymmetrical Rotor Slots," in Proceedings of *International Conference on Electrical Machines and Systems (ICEMS'12)*, Sapporo, Japan, Oct. 2012.

A.7 Publication VII

A. Stening, U. Shaukat and C. Sadarangani, "New Design Options For Induction Machines Using Modulated Rotor Slots," submitted for review to *IEEE Transactions on Energy Conversion*.